JOURNAL OF MATERIALS SCIENCE 33 (1998) 1555–1562

Estimation of creep crack growth rate in IN-100 based on the Q^* parameter concept

A. TOSHIMITSU YOKOBORI Jr, TOMOHARU UESUGI
Faculty of Engineering, Tohoku University, Aoba Aramaki, Aobaku, Sendai City 980-77, Japan

TAKEO YOKOBORI
School of Engineering and Science, Teikyo University, 1-1 Toyosatodai, Utsunomiya, Tochigi 320, Japan

AKIO FUJI, MASAKI KITAGAWA, ISAMU YAMAYA
Metallurgy Department, Research Institute, Ishikawajima-Harima Heavy Industries Co. Ltd, 3-2-16 Toyosu, Koutoku, Tokyo 135, Japan

MASAAKI TABUCHI, KŌICHI YAGI
National Reserach Institute for Metals, 1-2-1 Sengen, Tsukuba City, Ibaraki 305, Japan

Since the high-strength Ni-based superalloy, cast IN-100, is considered to be brittle at high temperatures, the stable creep crack growth region is limited. Therefore, technically, it is very difficult to perform creep tests and there are few experimental results on the creep crack growth behaviour of this material. We performed creep crack growth tests using Ni-based superalloy, cast IN-100, and derived the Q^* parameter for this material, which characterizes the creep crack growth rate. Using this Q^* parameter, we derived a law for the creep rupture life of this material. © *1998 Chapman & Hall*

1. Introduction

Since the high-stength Ni-based superalloy, cast IN-100, is considered to be brittle at high temperatures, the stable creep crack growth region is limited. Therefore, technically, it is very difficult to perform creep tests and there are few experimental results on the creep crack growth behaviour of this material [1–3]. For this material, the stress intensity factor is considered to be a mechanically determinate factor of creep crack growth behaviour. However, since detailed experimental results have not yet been accumulated, a systematic effect of stress and temperature on creep crack growth behaviour has not yet been obtained. Therefore, a mechanical test method was constructed to estimate the creep crack growth rate for Ni-based superalloy, cast IN-100 [4, 5]. This method was based on that for high-temperature ductile materials such as Cr–Mo–V steel [6].

In this paper, on the basis of this test method, we performed a creep crack growth test using cast IN-100 and derived the Q^* parameter for this material. Using the Q^* parameter, we derived an expression for the creep fracture life of this material.

2. Materials, specimens and experimental procedure

The alloy used is the Ni-based superalloy, cast IN-100. Its chemical composition and mechanical properties are shown in Tables I and II, respectively. The cubic γ' phase was observed in the virgin materials [4, 5]. The test specimens were of the compact tension (CT) type, as shown in Fig. 1. After individual precision casting, the test specimens were heat-treated and machined. The width, W, was usually 50.8 mm and the thicknesses, B, were 6.35, 12.7 and 25.4 mm. Fatigue precracks about 3 mm long were introduced at the tips of machined notches using an electrohydraulic fatigue testing machine at room temperature. All tests were performed using a lever-arm high-temperature creep-testing machine. The experimental conditons used at Tohoku University are shown in Table III. Experimental results at Ishikawajima-Harima Heavy Industries (IHI) and the National Research Institute of Metals (NRIM) were also included to estimate the creep crack growth behaviour of IN-100.

The crack length was measured by an electrical potential method and calculated using Johnson's [7] formula

$$a = \frac{2W}{\pi} \cos^{-1} \left[\frac{\cosh(\pi y_0/2W)}{\cosh(U/U_0) \cosh^{-1} \{[\cosh(\pi y_0/2W)]/[\cos(\pi a_0/2W)]\}} \right] \quad (1)$$

where a (mm) is the length of the crack, a_0 (mm) is the initial crack length, W (mm) is the width of the specimen, y_0 (mm) is the half-length between the terminals, U (μV) is the electrical potential and U_0 (μV) is the

TABLE I Chemical compostition of the material (mass %)

Element	Amount (mass %)	Element	Amount (mass %)
C	0.15	P	0.003
Si	0.01	S	0.001
Mn	0.01	B	0.013
Cr	8.51	N	0.0007
Mo	2.98	O	0.0007
Ti	4.77	Mg	0.0022
Al	5.68	Pb	< 0.0001
Co	13.47	Bi	< 0.00002
Fe	0.04	Se	< 0.0001
Zr	0.038	Te	< 0.00005
V	0.79	Tl	< 0.00005
		Ni	Balance

TABLE II Mechanical properties of the material

Temperature (°C)	Tensile stress (MPa)	0.2% proof stress (MPa)	Elongation (%)
25	918	781	5.9
25	1000	787	8.0
732	1026	861	7.3
850	858	605	5.9

initial voltage. (The thermoelectric potential is excluded from both U and U_0).

To maintain the centring, the specimens were heated by applying 10% of the test load. The specimens were held at the testing temperature for about 16 h and then loaded immediately with great care to avoid shock. The load line displacement was measured to determine creep deformation.

A schematic illustration at the testing machine and a photograph of the actual testing machine are shown in Figs 2 and 3, respectively. Details of the experimental method were given in our previous paper [6].

3. Experimental results

3.1. Estimation of creep crack growth rate

We adopted the stress intensity factor, K, the C^* parameter [8–12], the load line displacement rate, $\dot{\delta}$, [7, 14] and the Q^* parameter [13–17] as estimation parameters of the creep crack growth rate (CCGR). K is given by the following equation, according to

TABLE III Test conditions and symbols (W = 50.8 nm) (Tohoku University)

B (mm)	Temperature (°C)	Load (N)	Symbol used in Figs 4, 5, 9
6.35	800	6004	▲
6.35	825	5978	◮
6.35	850	6213	△
12.7	732	17304	□
12.7	732	16117	■
25.4	800	25402	●
25.4	825	25558	◐
25.4	825	24500	◑
25.4	825	22720	◓
25.4	850	25642	○
25.4	850	24500	◌

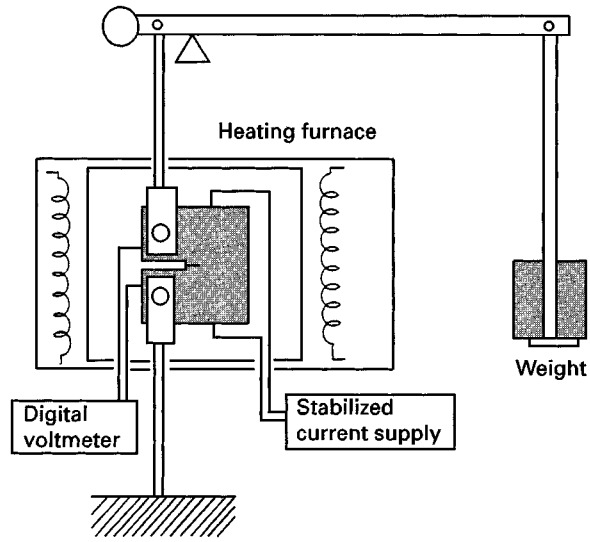

Figure 2 Schematic illustration of creep-testing machine.

ASTM E-399 [18]:

$$K = \frac{P}{BW^{1/2}} \frac{2 + a/W}{(1 - a/W)^{3/2}} f\left(\frac{a}{W}\right) \quad (2)$$

where

$$f\left(\frac{a}{W}\right) = 0.886 + 4.64\frac{a}{W} - 13.32\left(\frac{a}{W}\right)^2 + 14.72\left(\frac{a}{W}\right)^3 - 5.6\left(\frac{a}{W}\right)^4$$

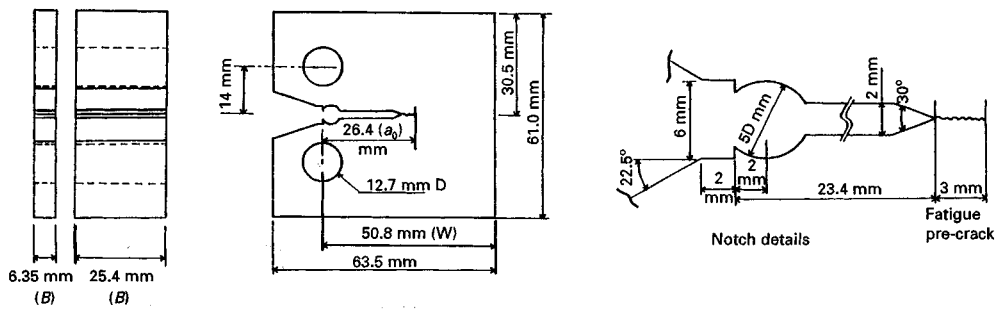

Figure 1 Geometry and size of CT specimens.

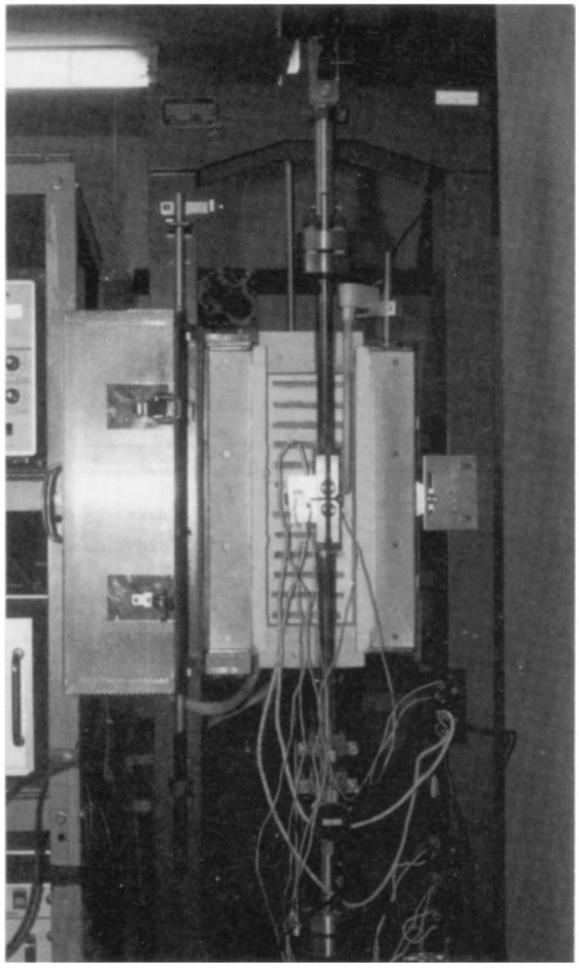

Figure 3 Lever-arm high-temperature creep-testing machine.

and P (N) is the load, B is the specimen thickness, W is the specimen width and a is the crack length. C^* is given by [19]

$$C^* = \frac{n}{n+1}\frac{P\dot{\delta}}{B\,b}\left(\gamma - \frac{\beta}{n}\right) \tag{3}$$

where

$$\gamma = \frac{2(1+\alpha)(1+a/W)/(1+\alpha^2) + \alpha\,(1-a/W)}{(1+a/W) + \alpha(1-a/W)} \tag{4}$$

$$\beta = \frac{\alpha}{\alpha + (1+a/W)/(1-a/W)}$$

$$\alpha = \left[\left(\frac{2a}{b}\right)^2 + 2\left(\frac{2a}{b}\right) + 2\right]^{1/2} - \left(\frac{2a}{b} + 1\right) \tag{5}$$

where $\dot{\delta}$ is the load line displacement rate, n is the stress-dependent coefficient of creep deformation and $b = W - a$.

Q^* for IN-100 is derived in Section 3.3

3.2. Estimation using C^* and $\dot{\delta}$

The CCGRs evaluated in terms of C^* and $\dot{\delta}$ are shown in Figs 4 and 5. Although both parameters apparently characterize the CCGR by a unique band independent of temperature and applied gross stress, the characteristics bands occupy only about 10% of the total creep fracture life, which corresponds to the final fracture region.

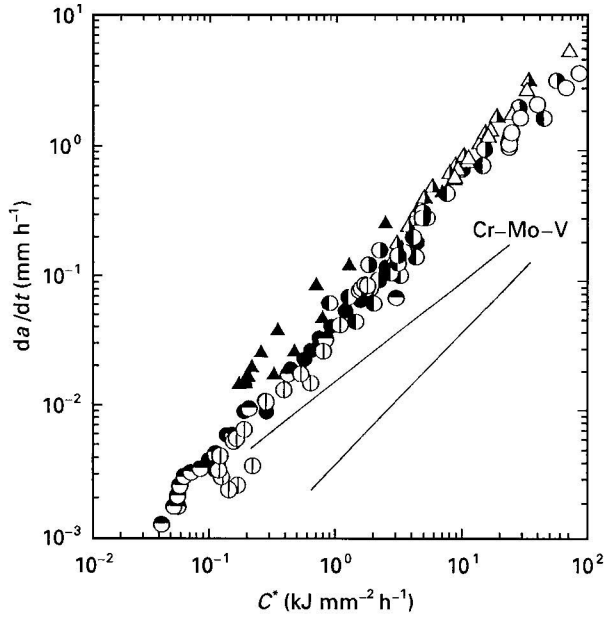

Figure 4 CCGR versus C^* for IN-100 at 800–850°C. (W = 50.8 mm). See Table III for explanation of symbols.

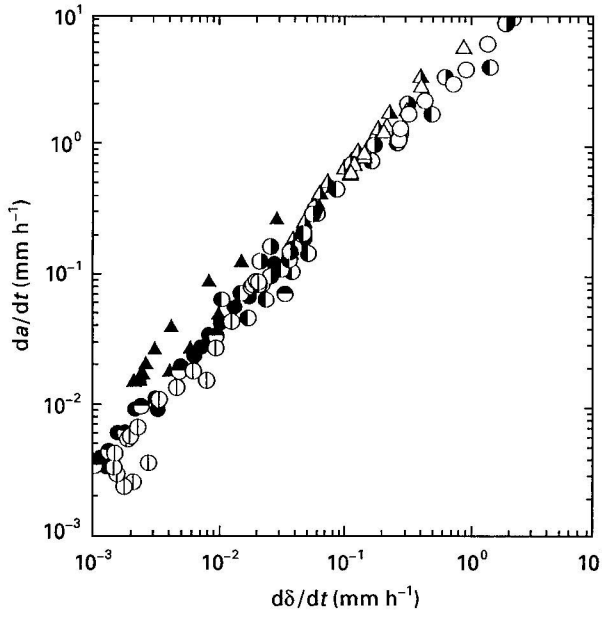

Figure 5 CCGR versus load line displacement rate for IN-100 at 800–850°C. (W = 50.8 mm). See Table III for explanation of symbols.

The creep fracture life mainly consists of the hold region H, as shown in Fig, 6. This is because for IN-100 alloys the process of constant CCGR accompanied by an accelerated process of CCGR occupies the main part of the total creep fracture life, as shown in Fig. 7, i.e. 80% of the total fracture life in this figure. We define this process as the first region of CCGR (linear region), which corresponds to the hold region H in Fig. 6. In this region, the creep elongation rate is also constant as in Fig. 8. These characteristcs are different from those of high-temperature creep ductile materials such as Cr–Mo–V steel, for which the accelerated CCGR occupies the main part of the total creep fracture life, as shown in Fig. 7. Therefore, it is

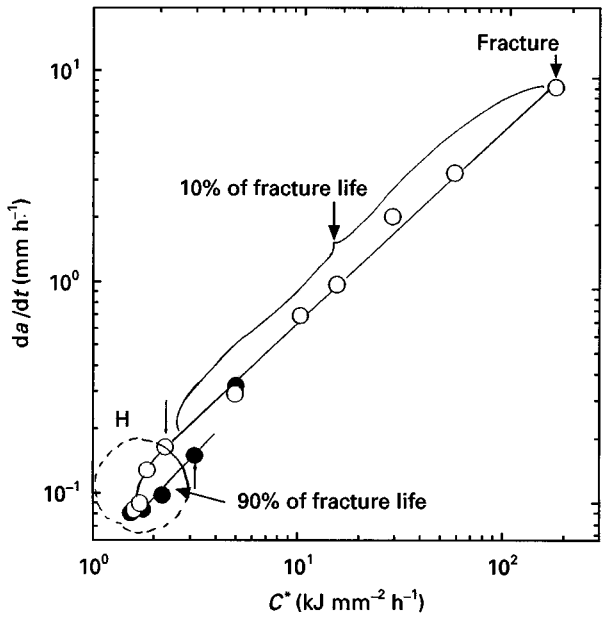

Figure 6 Dual-part behaviour of the relationship between CCGR and C^* for IN-100 ($B = 25.4$ mm; $T = 875$°C; $P = 24\,500$ N, NOSG). (●), C^* decreasing; (○), C^* increasing.

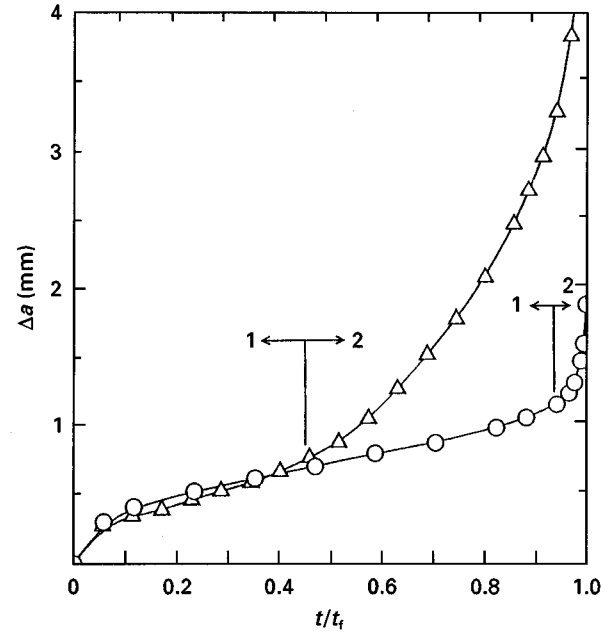

Figure 7 Creep crack extension curves for IN-100 alloy (○) and Cr–Mo–V steel (Δ)

important to determine the first region of the CCGR in order to estimate the creep fracture life for such high-temperature brittle materials.

3.3. Estimation using K

The CCGR was plotted against the stress intensity factor, as shown in Fig. 9. First, we discuss the CCGR characteristics for specimens with $B = 6.35$ mm. These experiments were performed with the same initial stress intensity factor. The results show that the CCGR increases with increasing temperature. Next, from experimental results for specimens with $B = 25.4$ mm at 825 °C, the CCGR is found to

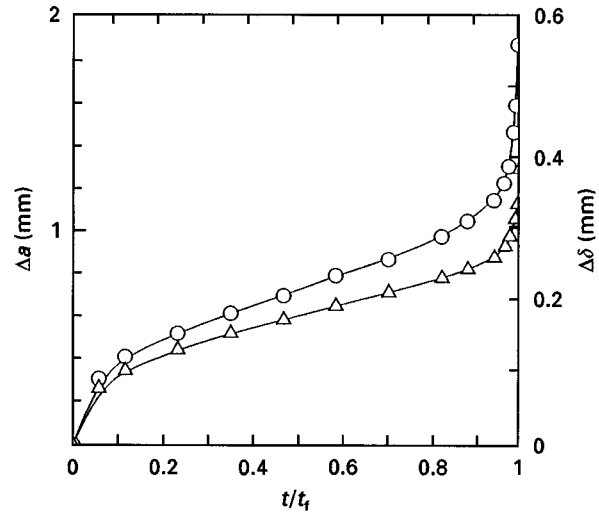

Figure 8 The relationship between the creep extension curve and the load line displacement curve (○), Δa; (△), $\Delta\delta$.

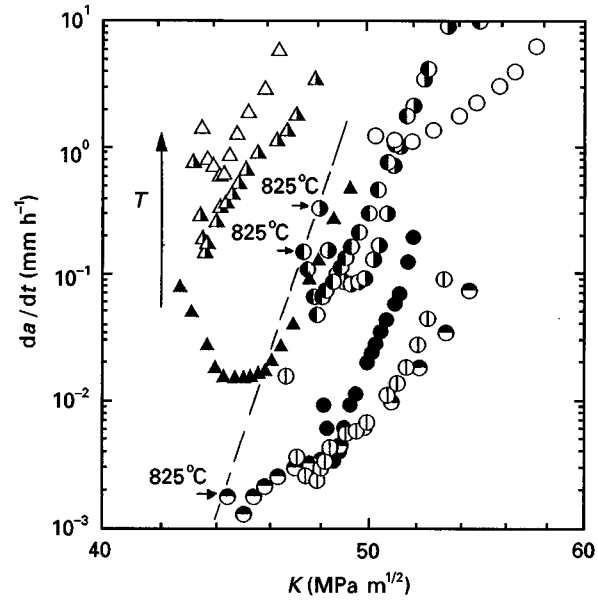

Figure 9 CCGR versus stress intensity factor for IN-100 at 800–850°C. ($W = 50.8$ mm). See Table III for explanation of symbols.

increase with increasing initial stress intensity factor, independent of the applied load.

As described in Section 3.2, the first region of the CCGR occupies the main part of the creep rupture life and its rate is constant. Therefore, it is important to estimate the first region of the CCGR for the initial stress intensity factor, K_{in}.

These results shows that the CCGR of IN-100 is determined by K_{in} and the temperature.

3.4. Derivation of the Q^* parameter

The concept of the Q^* parameter is shown in Fig. 10. Q^* was derived to estimate the CCGR based on thermally activated process theory [15–17]. The main purpose of Q^* is for use in estimating the high-temperature mechanical performance of materials and in predicting creep fracture life.

First, Q^* was applied to high-temperature ductile materials [13–17]. In this work, the derivation of Q^* for high-temperature brittle materials was performed.

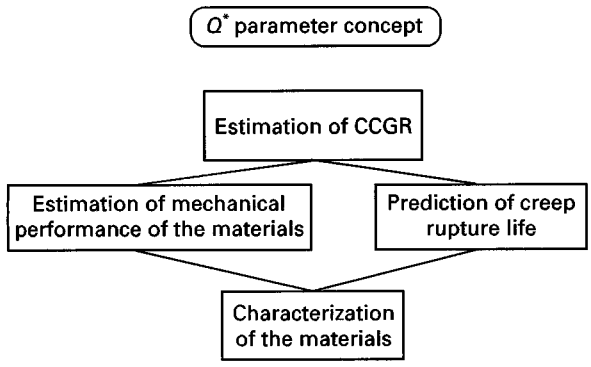

Figure 10 The concept and aim of the Q^* parameter.

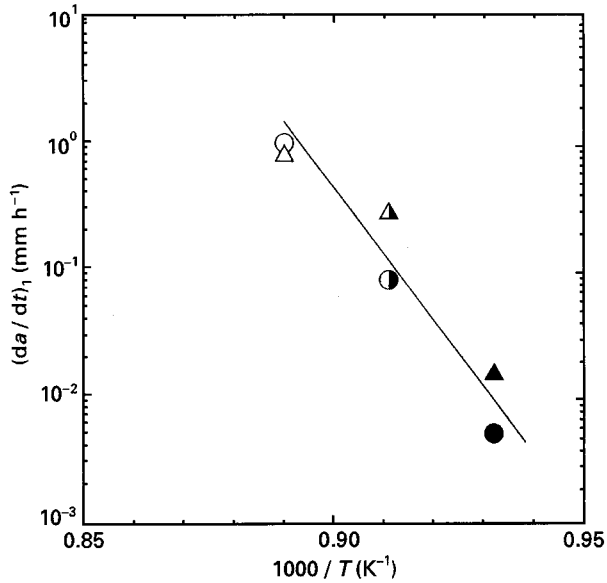

Figure 11 The relationship for IN-100 between CCGR and the inverse values of the absolute temperature for the first region. (W = 50.8 mm). See Table III for explanation of symbols.

The relationship between CCGR in the first region, $CCGR_1$, and the temperature is shown in Fig. 11. These results indicate that the CCGR is dominated by a thermally activated process. Furthermore, $CCGR_1$, is dominated by the initial stress intensity factor, K_{in}. The relationship between $CCGR_1$ and K_{in} is shown in Fig. 12. From these results, $CCGR_1$, i.e., $(da/dt)_1$ (mm h^{-1}) is given by

$$\left(\frac{da}{dt}\right)_1 = A\, g(B)\, K_{in}^{63.8} \exp\left(-\frac{Q}{RT}\right) \quad (6)$$

where A is a constant, $g(B)$ is a function of the specimen thickness, T is the absolute temperature, Q is an activation energy equal to 1106.4 KJ mol^{-1} and R is the gas constant.

For specimens with a thickness of 25.4 mm,

$$\left(\frac{da}{dt}\right)_1 = 1.26 \times 10^{-56}\, K_{in}^{63.8} \exp\left(-\frac{1106.4}{RT}\right) \quad (7)$$

By taking logarithms of both sides of Equation (7) and substituting in the gas constant, we obtain

$$\log\left(\frac{da}{dt}\right) = -55.9 + \left(63.8 \log K_{in} - \frac{57.79}{T} \times 10^3\right) \quad (8)$$

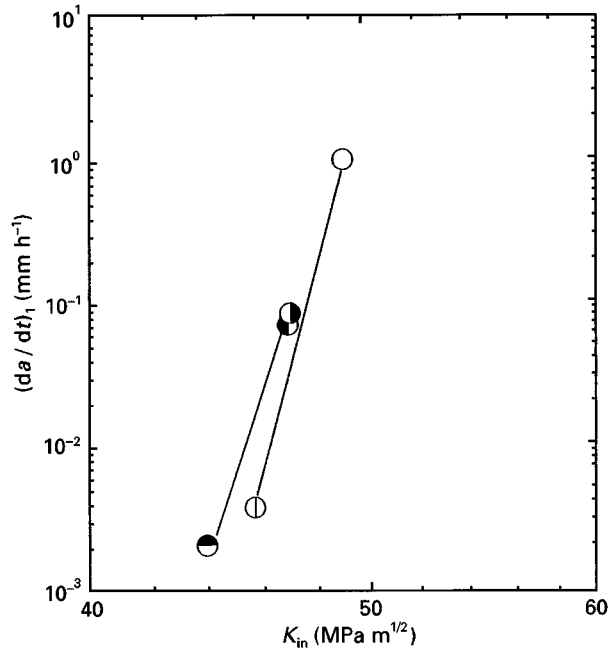

Figure 12 The relationship for IN-100 between CCGR and the initial stress intensity factor for the first region. (W = 50.8 mm). See Table III for explanation of symbols.

TABLE IV Test conditions and symbols (W = 50.8 mm) (IHT, NRIM and Tohoku University)

B (mm)	Temperature (°C)	Load (N)	Symbol used in Fig. 13	Laboratory
6.35	732	7435	▲	IHI
6.35	825	6472	◭	
12.7	732	15004	■	
12.7	800	12503	◧	
12.7	825	11072	◨	
12.7	850	12033	◓	
12.7	850	12503	◒	
25.4	732	30106	●	
25.4	800	24614	◐	
6.35	850	5657	◭	NRIM
6.35	850	5419	◬	
25.4	850	20367	◑	
6.35	800	6004	◬	Tohoku
6.35	825	5978	◬	University
6.35	850	6213	△	
12.7	732	17304	■	
12.7	732	116117	□	
25.4	800	25402	◓	
25.4	825	25558	◒	
25.4	825	24500	⊕	
25.4	825	23834	⊗	
25.4	850	25642	○	
25.4	850	24500	●	

Therefore, Q^* for the first region of the CCGR is given by

$$Q^* = 63.8 \log K_{in} - \frac{57.79}{T} \times 10^3 \quad (9)$$

The experimental results obtained in our three laboratories (Table IV) under various conditions are

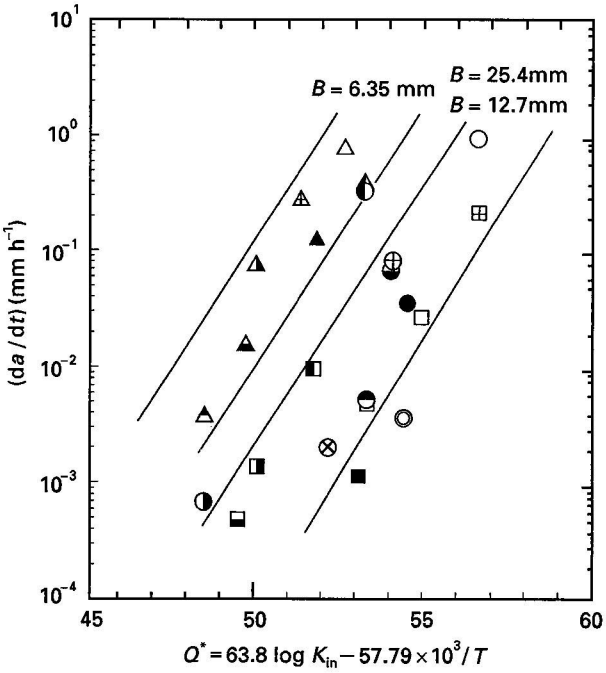

Figure 13 The relationship between CCGR and the Q^* parameter (W = 50.8 mm). See Table IV for explanation of symbols.

plotted against Q^* in Fig. 13. These results show that Q^* can be used to estimate the CCGR of IN-100 accurately in the first region for $B \geqslant 12.7$ mm.

The CCGR of a thin plate specimen (B = 6.35 mm) is greater than those of specimens with other thicknesses (B = 12.7 and 25.4 mm). This is due to the effect of the microstructure of the thin specimen. As described in Section 2, these specimens were fabricated by individual precision casting followed by heat treatment and machining. The microstructure of the specimen 6.35 mm thick is different from those of specimens of other thicknesses (B = 12.7 and 25.4 mm), as shown in Fig. 14 [4, 5]. This is why the CCGR of the specimen 6.35 mm thick is different from those of specimens with other thicknesses.

Therefore, if the microstructures of the materials are similar, Q^* can be used to estimate the CCGR of IN-100 in the first region for various temperatures, applied loads and specimen thickness conditions.

3.5. Expression for creep rupture life based on Q^*

By integrating Equation 7, we obtain an expression for the creep fracture life:

$$\int_0^{t_f} dt = \int_{a_i}^{a_f} \frac{\exp(Q/RT)}{AK_{in}^n} da \tag{10a}$$

$$t_f = \frac{a_f - a_i}{A} \exp\left(\frac{Q}{RT}\right) \frac{1}{K_{in}^n} \tag{10b}$$

where A is a constant, a_i (mm), is the initial crack length, a_f (mm) is the final crack length, n = 63.8 and t_f (h) is the creep fracture life.

If we define the creep fracture life as the time at which the value of $(a_f - a_i)$ takes some specified value, C_1 (constant), then we obtain

$$\ln K_{in} = \frac{1}{n} \ln\left(\frac{C_1}{A}\right) - \frac{1}{n}\left(\ln t_f - \frac{Q}{RT}\right) \tag{11}$$

where $(1/n) \ln (C_1/A)$ is a constant. The experimental relationship between $\log K_{in}$ and $(\ln t_f - Q/RT)/n$ is

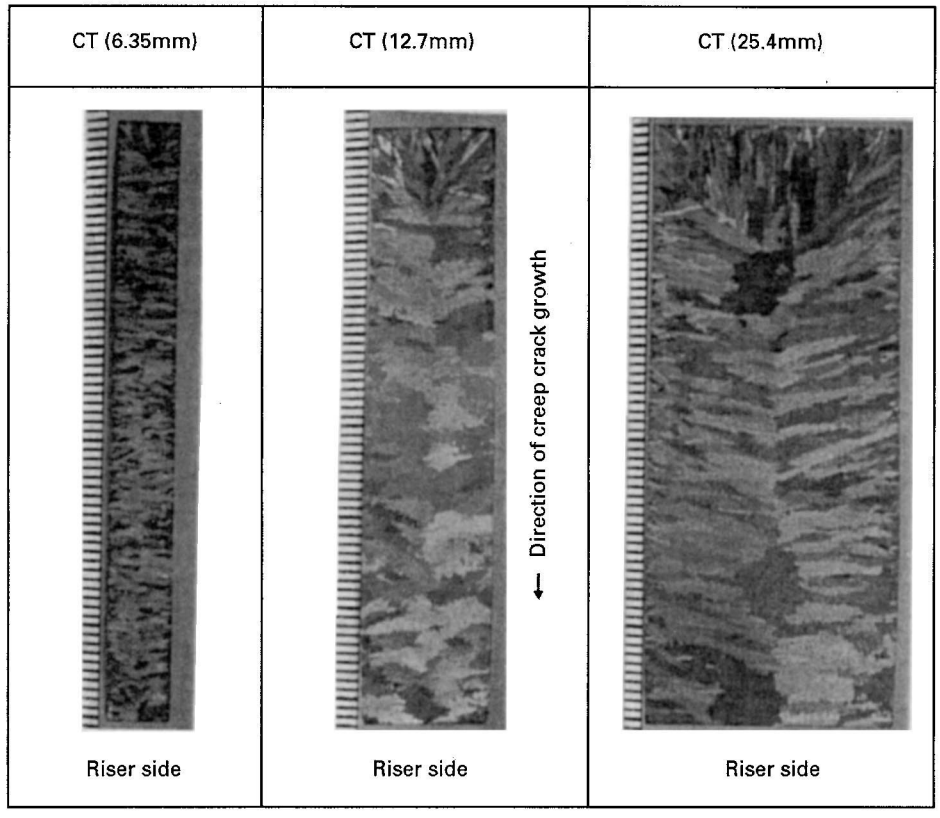

Figure 14 Microstructures of the specimen 6.35 mm thick and other thick specimens.

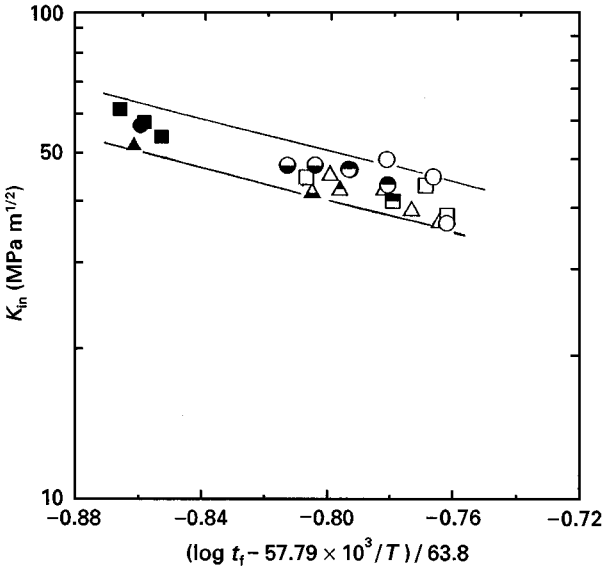

Figure 15 Master curve for the estimation of the creep rupture life for IN-100.

	Symbol		
T (°C)	B = 6.35 mm	B = 12.7 mm	B = 25.4 m,m
732	▲	■	●
800	◭	◨	◒
825	△	◧	◓
850	△	□	○

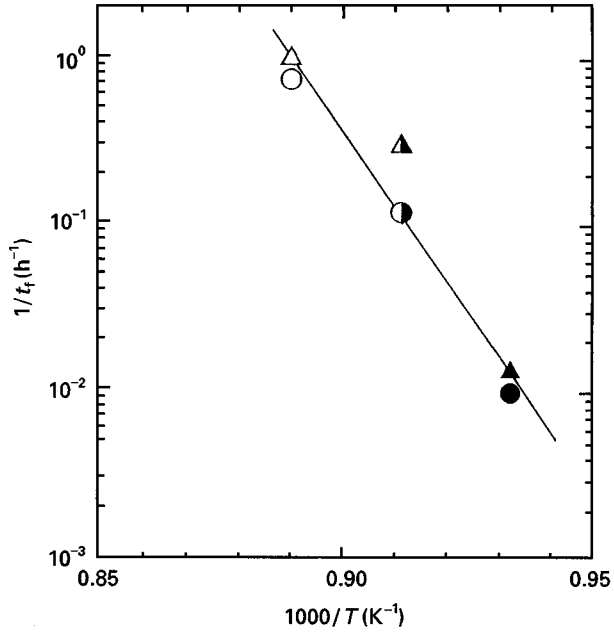

Figure 16 The relationship between the inverse values of the creep rupture life and the absolute temperature for IN-100. (W = 50.8 mm). See Table III for explanation of symbols.

shown in Fig. 15. These results show that the experimental results for CCGR at all temperatures, applied loads and specimen thicknesses can be estimated by a unique characteritic curve, and that the creep fracture life is dominated by the temperature and initial stress intensity factor.

4. Discussion

The CCGR of the specimen 6.35 mm thick is higher than those of specimens with greater thickness, as shown in Fig. 13. However, Equation 11 based on the Q^* parameter can be used to estimate the creep fracture life for all specimens because of the unique characteristic master curve, including that of the specimen 6.35 mm thick as shown in Fig. 15. This is due to the following reason.

In this estimation method, we paid particular attention to the first region in which the CCGR is constant, since the second region, in which the CCGR increases non-linearly, does not affect the total creep fracture life much. However, in cases where the first region has a high CCGR, such as that of the specimen 6.35 mm thick, the transition time from the first region to the second region of the CCGR becomes shorter and the ratio of the fracture life corresponding to the second region to the total fracture life increases. Therefore, the effect of the increase in the CCGR in the first region on the total creep fracture life is cancelled because of the increase in the effect of the second region on the total creep fracture life.

The inverse, $1/t_f$, of the creep fracture life has similar characteristics to the CCGR in the first region, as shown in Figs 11 and 16. Therefore, it is reasonable to conclude that this first region of CCGR dominates the total creep fracture life.

These findings are different from the characteristics of ductile materials, such as Cr–Mo–V steel, which are determined by the second region of CCGR.

In the first region of the CCGR, CCGR and the displacement rate, $d\delta/dt$ are constant. Therefore, when the CCGR is estimated using C^*, which is determined by $d\delta/dt$, the relationship between the CCGR and C^* in the first region is localized in the hold region, as shown in Fig. 6. This results in difficulty in estimating the CCGR using C^* in this region.

For In-738 and IN-939, Nazmy and Wuthrich [2] showed that the CCGR in the acceleration region is controlled by a thermally activated process and can be estimated in terms of the stress intensity factor and the temperature. However, in this work, it is not clear whether this acceleration region constitutes the main part of the total creep fracture life or not. Furthermore, the experimental relationship between the CCGR and the stress intensity factor for various temperatures does not show typical characteristics of a thermally activated process. Therefore, for these materials, it is also important to focus on the first region of the CCGR. For Ni-based superalloys, the proposed type of Q^* parameter can be used to estimate the CCGR in the first region and the total creep fracture life.

The physical meaning of the activation energy for the CCGR of this material should be clarified in relation to the strengthening mechanism due to the cubic γ' precipitated phase structure. However, for this precipitate-strengthened material, the activation energy of the CCGR is not always equal to that of the creep elongation rate of a smooth specimen which is different from the case of matrix-strengthened materials, because the effect of the interaction between the creep

crack and the γ' phase on the crack growth is dominant instead of the void formation at the grain boundary.

5. Conclusions

1. For IN-100 alloys, the region of constant CCGR accompanied by accelerated CCGR constitutes the main part of the total creep fracture life. The CCGR is determined by the initial stress intensity factor, K_{in}, and the temperature. These properties are characteristics of high-temperature creep brittle materials and are different from those of high-temperature creep ductile materials, such as Cr–Mo–V steel.
2. The Q^* parameter in the constant CCGR region was derived for IN-100. This parameter can be used as the Q^* parameter for high-temperature brittle materials.
3. By integrating Q^*, an expression for the creep fracture life was derived for a cracked IN-100 specimen.
4. For Ni-based superalloys, the proposed Q^* parameter can be used to estimate the creep crack growth rate in the first region and the total creep fracture life.

Acknowledgements

Acknowledgement should be made to the financial grant in-aid from the Science and Technology Agency for the TWA19 of VAMAS Project, and also to the Japan Society for Promotion of Science Committee 129 Project, including the support of VAMAS activities. Among the Committee, the following members should be thanked: Professor Ryuji Miyata, Nagoya University; Associate Professor Shinji Konosu, Ibaraki University; Dr Tadao Iwadate, Nippon Steel Works Ltd; Dr Hironori Kino, Mitsubishi Heavy Industrial Ltd; Dr Masao Shiga, Hitachi Research Laboratory, Hitachi Ltd; Dr Takao Inukai, Toshiba Corporation Ltd; Dr Kenji Kikuchi, Japan Atomic Energy Agency, Tokai Research Institute.

References

1. R. C. DONATH, T. NICHOLAS and L. S. FU, ASTM Special Technical Publication 743 (1981) p. 186.
2. M. Y. NAZMY and C. WUTHRICH, Mater. Sci. Eng. **61** (1983) 119.
3. N. E. ASHBAUGH, ASTM Special Technical Publication 791 (American Society for Testing and Materials, Philadelphia, PA, 1983) p. 517.
4. A. FUJI and M. KITAGAWA, in Mechanical Behaviour of Materials, Proceedings of the Sixth International Conference on Magnetism, Vol. 2, edited by M. Jono and T. Inoue, Pergamon Press (1991) p. 93.
5. *Idem.*, in "Advances in fracture resistance and structural integrity", Proceedings of the Eighth International Conference on Fracture, edited by V.V. Panasyuk *et al.* (Pergamon, Oxford, 1994) p. 487.
6. T. YOKOBORI, C. TANAKA, K. YAGI, M. KITAGAWA, A. FUJI, A. T. YOKOBORI Jr and M. TABUCHI, *Mater. High Temp.* **10** (1992) 97 (Errata, *ibid.* **10** (1992) 224).
7. H. H. JOHNSON, *Mater. Res. Stand.* **5** (1965) 442.
8. J. R. RICE, *J. Appl. Mech.* **35** (1968) 379.
9. K. OHJI, K. OGURA and S. KUBO, *Japan Soc. Mech. Engng* **44** (1975) 183.
10. J. R. LANDES and A. J. BEGLEY, in "Mechanics of crack growth", ASTM Special Technical Publication 590 (American Society for Testing and Materials, Philadelphia, PA, 1976) p. 128.
11. R. KOTERAZAWA and T. MORI, *J. Engng Mater. Technol.* **99** (1977) 298.
12. S. TAIRA, R. OHTANI and T. KITAMURA, *ibid.* **101** (1979) 154.
13. A. T. YOKOBORI Jr, T. YOKOBORI, H. TOMIZAWA and H. SAKATA, Trans. ASME, J. Eng. Mater. Technol. **105** (1983) 13.
14. A. T. YOKOBORI Jr, T. YOKOBORI, T. KURIYAMA, T. KAKO and Y. KAJI, in Proceedings of the JSME–IMechE–ASME–ASTM Conference on Creep (1986) p. 135.
15. A. T. YOKOBORI Jr and T. YOKOBORI, in "Advances in fracture research", Proceedings of the Seventh International Conference on Fracture, Vol. 2, edited by K. Salama *et al.* 2. (1989) 1723 Pergamon Press.
16. A. T. YOKOBORI Jr, T. YOKOBORI, T. NISHIHARA and T. YAMAOKU, *Mater. High Temp.* **10** (1992) 108 (Errata, *ibid.* **10** (1992) 224).
17. A. T. YOKOBORI Jr and T. YOKOBORI, in "Creep and fracture of engineering materials and structures", edited by B. Wilshire and R.W. Evans (Institute of Materials, London, 1993) p. 81.
18. ASTM Standard E-399 (American Society for Testing and Materials, Philadelphia, PA, 197).
19. A. SAXENA, H. A. ERNST and J. D. LANDES, *Int J. Fract.* **23** (1983) 245.

Received 14 January
and accepted 14 October 1997